Received: 7 November 2017 | Revised: 15 December 2017 | Accepted: 19 December 2017
DOI: 10.1002/aoc.4271

FULL PAPER

WILEY Applied Organometallic Chemistry

# An efficient and new protocol for the Heck reaction using palladium nanoparticle-engineered dibenzo-18-crown-6-ether/MCM-41 nanocomposite in water

Maedeh Azaroon[1] | Ali Reza Kiasat[1,2]

[1] Chemistry Department, College of Science, Shahid Chamran University of Ahvaz, Ahvaz, Iran

[2] Petroleum Geology and Geochemistry Research Centre (PGGRC), Shahid Chamran University of Ahvaz, Ahvaz, Iran

**Correspondence**
Maedeh Azaroon, Chemistry Department, College of Science, Shahid Chamran University of Ahvaz, Ahvaz, Iran.
Email: m-azaroon@phdstu.scu.ac.ir

Palladium nanoparticle-incorporated mesoporous organosilica (MCM-41-Crown.Pd) was synthesized via the grafting of dibenzo-18-crown-6-ether moieties on the MCM-41 surface, followed by reaction of the nanocomposite with palladium acetate and then its reduction in ethanol. The cavity of the immobilized dibenzo-18-crown-6 as host material can stabilize the palladium nanoparticles effectively and prevent their aggregation and separation from the surface. The structure of the nanocomposite was characterized using various techniques. The catalytic properties of the nanocomposite in the Heck coupling reaction, one of the most useful transformations in organic synthesis, between aryl halides and olefins in water were also explored. The main advantages of the method are low cost, high yields, easy work-up and short reaction time. The nanocatalyst can be easily separated from a reaction mixture and was successfully examined for seven runs, with a slight loss of catalytic activity.

**KEYWORDS**
Heck coupling reaction, heterogeneous nanocatalyst, MCM-41-Crown.Pd, Pd nanoparticle-incorporated mesoporous organosilica

## 1 | INTRODUCTION

The economic improvement of feasible materials and processes to eliminate harmful substances and toxic waste materials is of paramount importance to organic synthesis and environmental aspects.[1] Recently, in regards to this challenge, research has been focused on the synthesis and functionalization of mesoporous materials such as organic polymers, silica, zeolite, alumina, hydroxyapatite and clays as supports for homogeneous catalysts. Among these, MCM-41, because of its various advantages such as tunable pore size, controlled size, morphology and dual-functional surface (external and internal), has attracted a great deal of attention.[2,3]

Organometallic catalysts immobilized on mesoporous silica supports including MCM-41, SBA-15 and PMO exhibit significant improvement in the catalytic activity owing to the enhanced dispersion of active sites and faster diffusion of large organic molecules.[4–9] Furthermore, such functionalized silica is notable for its low toxicity, environmental friendliness and high chemical stability. These advantages can be developed by using water as a non-toxic and non-flammable solvent.[10–13]

The Pd-catalysed cross-coupling reactions, especially Heck arylation of olefins with aryl halides, are simple, efficient and versatile routes to the formation of carbon–carbon bonds commonly used in modern organic synthesis.[14–17] For excellent performance of Pd-catalysed processes, use of high-activity Pd catalysts and green reaction conditions are two important strategies for the design of new heterogeneous Pd catalytic systems.[18–22]

Pd nanoparticles in catalyst systems have some disadvantages, such as agglomeration due to their high surface energy and difficulty in separation from a reaction mixture due to the homogeneous character. Recently, using immobilized metal nanoparticles as heterogeneous catalysts has considerably expanded the scope and led to interesting applications.[23–29]

Many studies have been focused on Pd loaded on modified MCM-41, such as Schiff base anchored on MCM-41,[30–32] thioether-functionalized MCM-41,[33] thiol-functionalized MCM-41[34] and diphosphino-functionalized MCM-41.[22,35] However, to our knowledge, there has been no general study of the Heck reaction catalysed by a crown ether-functionalized MCM-41-anchored Pd (0) catalyst. Crown ethers are a class of macrocyclic ligands with high affinity and selectivity for alkali and alkaline earth metal ions.[36] Because of their hydrophobic exteriors and hydrophilic cores, they are typically appropriate moieties to make junctions with larger organic molecules.[37]

By considering all of the points mentioned above and in the course of our investigations into the development of novel inorganic–organic hybrid heterogeneous nanocatalysts in organic transformations, the aim of the work presented here was to highlight the synergistic effects of the combined properties of MCM-41, crown ether cavity and stabilizing of Pd nanoparticles. The catalytic properties of Pd nanoparticle-incorporated mesoporous organosilica, MCM-41-Crown.Pd, in Heck cross-coupling reactions were also investigated.

## 2 | EXPERIMENTAL

### 2.1 | General Remarks

Cetyltrimethylammonium bromide (CTAB; 98%), tetraethyl orthosilicate (TEOS; 98%), palladium(II) acetate ($Pd(OAc)_2$; 98%), absolute ethanol (99.8%), 3-aminopropyltrimethoxysilane (97%, Aldrich), aryl halides and other chemical materials were purchased from Fluka and Merck and used without further purification. The purity determination of the products and reaction monitoring were accomplished using TLC on silica gel polygram SILG/UV 254 plates. Products were characterized by comparison of their physical and spectral data with those reported in the literature.

The surface area and pore size distribution of the support were measured at 77 K using the nitrogen adsorption–desorption method (ASAP 2000, Micromeritics). All samples were degassed at 120 °C during 2 h before such measurements. Fourier transform infrared (FT-IR) spectra were recorded with a BOMEM MB-Series 1998 FT-IR spectrometer. Products were characterized using $^1H$ NMR and $^{13}C$ NMR spectra with known samples (S1–S6, supporting information). NMR spectra were recorded in $CDCl_3$ with a Bruker Advance DPX 400 MHz spectrometer using tetramethylsilane as the internal standard. X-ray diffraction (XRD) patterns of the catalyst were obtained using a Philips X-ray diffractometer (model PW 1840) with a wavelength of1.54056 Å, the diffraction angles ($2\theta$) being set between 1° and 80°. Scanning electron microscopy (SEM) was conducted using a MIRA3 FEG-SEM (TESCAN, 1–30 kV). An Analytik Jena (Germany) flame atomic absorption spectroscopy (AAS) instrument was used for determination of Pd. Energy-dispersive X-ray spectroscopy (EDS) analysis was conducted with a VEGA\\TESCAN-XMUT instrument. Transmission electron microscopy (TEM) images were obtained using a Zeiss EM10C (80 kV) instrument. Thermogravimetric analysis (TGA) was carried out with a BAHR SPA 503 under a nitrogen atmosphere at a heating rate of 10 °C $min^{-1}$. Mass spectra were obtained with an Agilent Technology ((HP) 5973 Network Mass Selective Detector) instrument at 70 eV.

### 2.2 | Preparation of MCM-41-Crown.Pd

#### 2.2.1 | Preparation of aminopropyl-grafted mesoporous MCM-41

Aminopropyl-grafted mesoporous MCM-41 was synthesized via surfactant-templated sol–gel methodology and then post-modification process. First, a mixture of CTAB (1 mmol, 0.4 g) and NaOH (2.54 mmol, 0.102 g) in water was heated at 80 °C for 30 min. When the pH reached 12.3, TEOS (8 mmol, 1.7 g) was slowly added and the reaction mixture stirred at 80 °C for 2 h. After quenching by cooling the solution to room temperature, MCM-41 silica was precipitated.[6]

For the grafting of aminopropyl moieties to the surface of MCM-41, 3-aminopropyltrimethoxysilane (10 mmol) was added to a suspension of MCM-41 (1 g) in anhydrous toluene (100 ml). The mixture was heated under reflux conditions for 24 h under argon protection. The light yellow solution was allowed to cool and was then collected by filtration, washed thoroughly with toluene and dried under vacuum to afford pure 3-aminopropyl-modified MCM-41. The surfactant (CTAB) was removed by acid extraction with concentrated HCl (1 ml) in methanol (100 ml) at 60 °C for 6 h.

#### 2.2.2 | Synthesis of 4′,4″-diformyldibenzo-18-crown-6-ether (DFBCE)

Diethylene glycol ditosylate (DEDT) was firstly synthesized and used as the precursor for the synthesis of benzo crown ether according to Pederson's method with suitable adaptation.[7,8] Briefly, for the preparation of DEDT,[9] diethylene glycol (140 mmol, 14.86 g) was dissolved in tetrahydrofuran (THF; 80 ml). Meanwhile, an aqueous solution of sodium hydroxide (400 mmol, 16 g) in water (80 ml) was prepared. The two solutions were mixed and cooled using an ice bath with magnetic stirring. To this mixture was added dropwise tosyl chloride (260 mmol, 48.6 g) in THF (80 ml) over 2 h with continuous stirring and cooling of the mixture below 5 °C. The solution was stirred at 0–5 °C for an additional 2 h. After this, the mixture was poured into ice–water (250 ml). The DEDT product was filtered, washed with distilled water, dried and recrystallized twice from methanol to afford a pure product.

Then for the synthesis of DFBCE, a mixture of 3,4-dihydroxybenzaldehyde (60 mmol, 8.28 g) and sodium

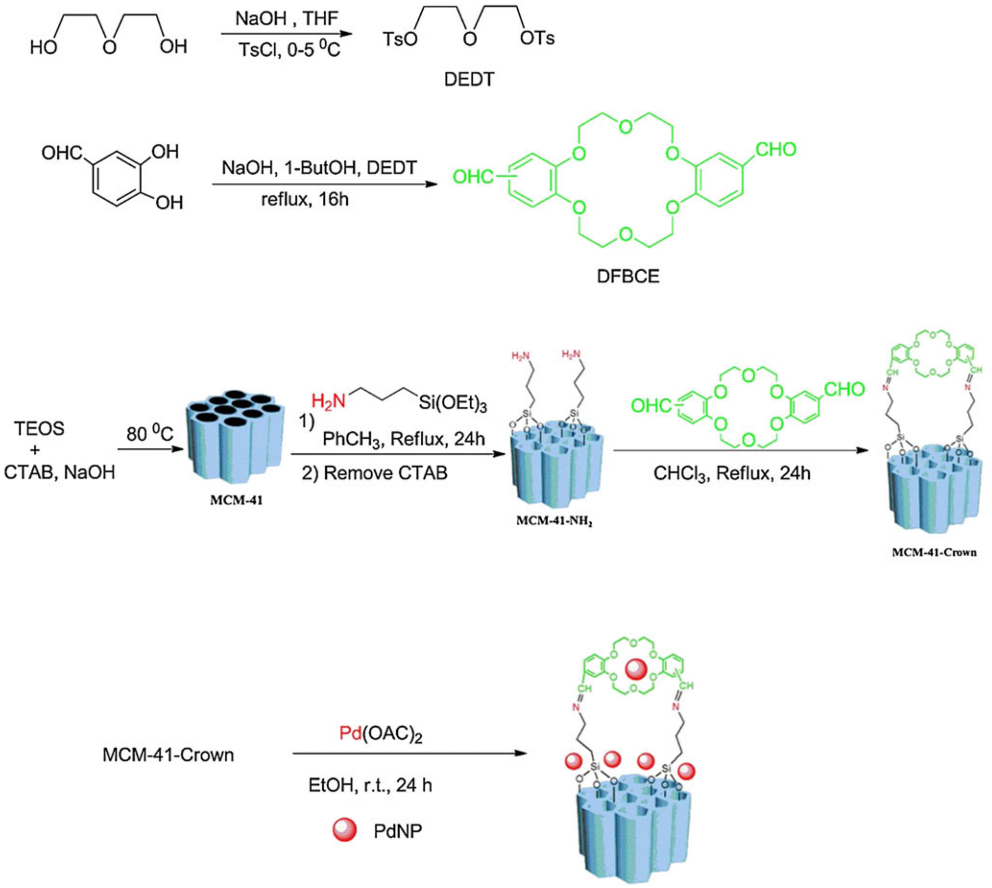

**SCHEME 1** Synthetic route for preparation of MCM-41-Crown.Pd.

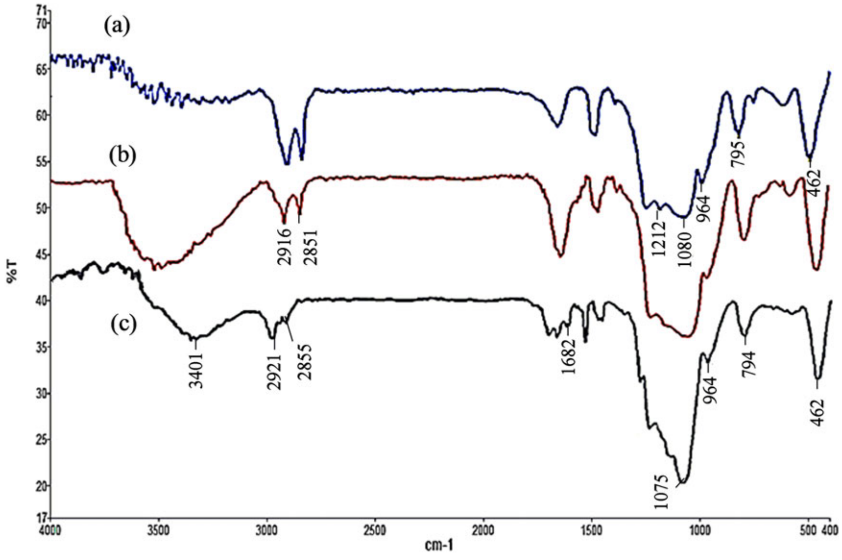

**FIGURE 1** FT-IR spectra of (a) MCM-41 with CTAB, (b) MCM-41-NH$_2$ and (c) MCM-41-Crown

hydroxide pellets (60 mmol, 2.44 g) in 1-butanol (40 ml) was refluxed under argon for 30 min to ensure complete dissolution of sodium hydroxide. A solution of DEDT (30 mmol, 12.36 g) in 1-butanol (20 ml) was added slowly over 1 h, and the mixture was refluxed for 1 h. The temperature was lowered to 90 °C and sodium hydroxide pellets (2.44 g) were added. Refluxing was continued for 30 min and DEDT (30 mmol, 12.36 g) in 1-butanol (20 ml) was added slowly over 1 h. Refluxing was continued for 16 h. Concentrated hydrochloric acid (1 ml) was slowly added, and then a third of the solvent was rapidly removed by distillation. The distillation was continued but the volume in the flask was kept constant by the steady addition of water until the vapour temperature reached 100 °C. The mixture was filtered, washed with 200 ml of water and sucked dry. The DFBCE product was dispersed in 200 ml of acetone, stirred for 30 min, filtered, washed with 50 ml of acetone and dried in an oven at 100 °C.

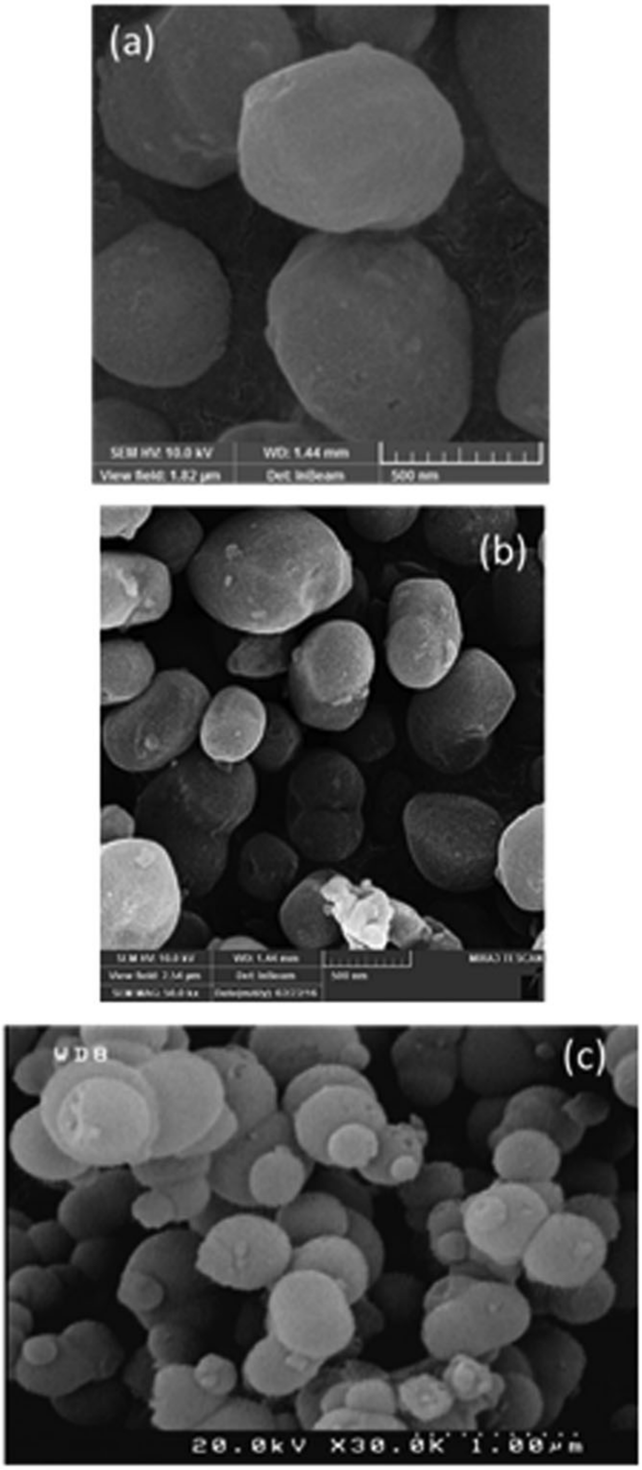

**FIGURE 2** SEM images of (a) MCM-41, (b) MCM-41-Crown and (c) MCM-41-Crown.Pd.

### 2.2.3 | Preparation of MCM-41-anchored dibenzo-18-crown-6-ether

DFBCE (1.5 mmol, 0.624 g) was dissolved in $CHCl_3$ (50 ml) and refluxed to complete dissolution of the crown ether. Aminopropyl-grafted mesoporous MCM-41 (1 g) was added to the mixture and refluxed for 24 h. The precipitate, MCM-41-Crown, was filtered, washed with dry $CHCl_3$ (3 × 20 ml) and dried in an oven at 50 °C for 4 h.

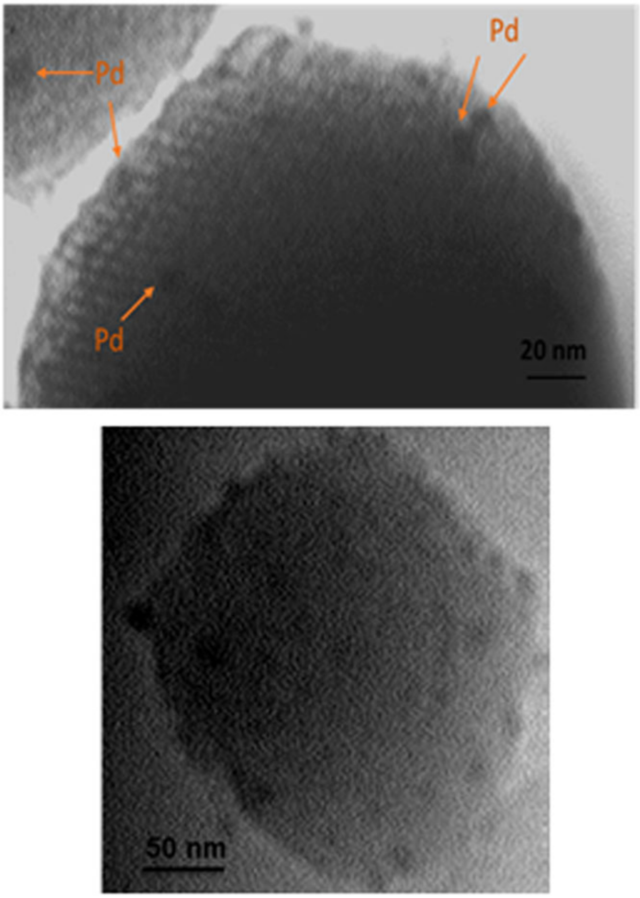

**FIGURE 3** TEM images of MCM-41-Crown.Pd.

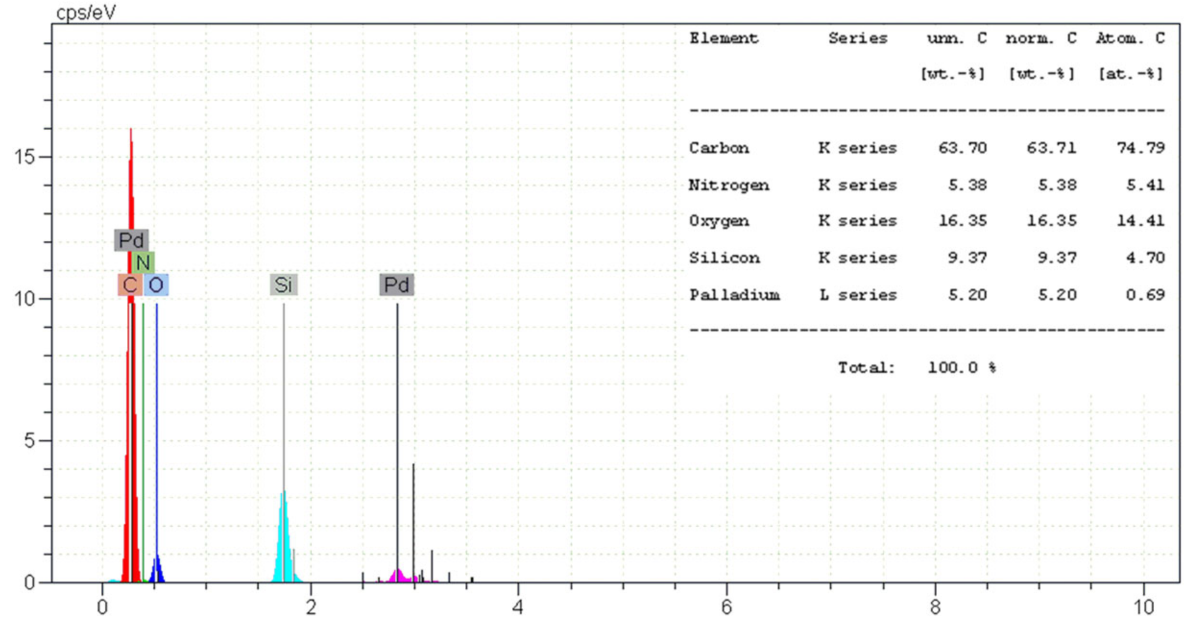

| Element | Series | unn. C [wt.-%] | norm. C [wt.-%] | Atom. C [at.-%] |
|---|---|---|---|---|
| Carbon | K series | 63.70 | 63.71 | 74.79 |
| Nitrogen | K series | 5.38 | 5.38 | 5.41 |
| Oxygen | K series | 16.35 | 16.35 | 14.41 |
| Silicon | K series | 9.37 | 9.37 | 4.70 |
| Palladium | L series | 5.20 | 5.20 | 0.69 |
| | Total: | 100.0 % | | |

**FIGURE 4** EDS spectrum of MCM-41-Crown.Pd.

### 2.2.4 | Incorporation of Pd nanoparticles into MCM-41-Crown

Palladium acetate (0.12 g, 0.52 mmol) was added to MCM-41-Crown (2 g) in absolute ethanol (20 ml), and stirred for 24 h at room temperature under argon protection. Then, the mixture was filtered and washed with ethanol (3 × 10 ml) and diethyl ether (3 × 10 ml). After drying in a vacuum oven at 80 °C overnight, the MCM-41-Crown.Pd (1.3 mol% Pd) catalyst was obtained as a dark solid.

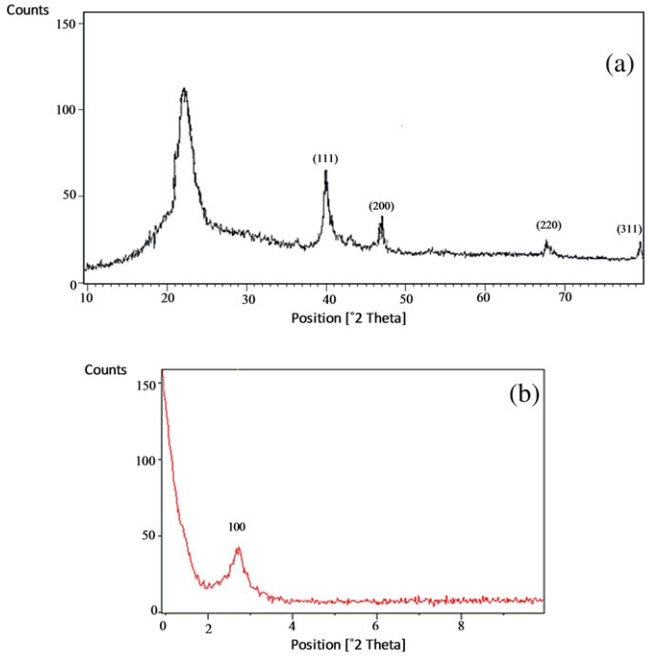

**FIGURE 5** (a) High-angle and (b) low-angle XRD patterns of MCM-41-Crown.Pd nanocomposite

## 2.3 | General Procedure for Heck Coupling Reaction Catalysed by MCM-41-Crown.Pd Nanocomposite in Water

In a typical experiment, to a mixture of aryl halide (1 mmol), styrene (1 mmol) and $K_2CO_3$ (2.5 mmol) in 5 ml of deionized water, MCM-41-Crown.Pd (0.07 g, 1.3 mol%) was added and heated in an oil bath (90 °C) for the required time. The reaction was monitored using TLC. After completion of the reaction, the mixture was cooled to room temperature and filtered, and the remaining solid was washed with $CH_2Cl_2$ (3 × 5 ml). After extraction, the organic layer was dried over $Na_2SO_4$ and evaporated under reduced pressure; the crude product was purified by silica gel chromatography (*n*-hexane–AcOEt as eluent).

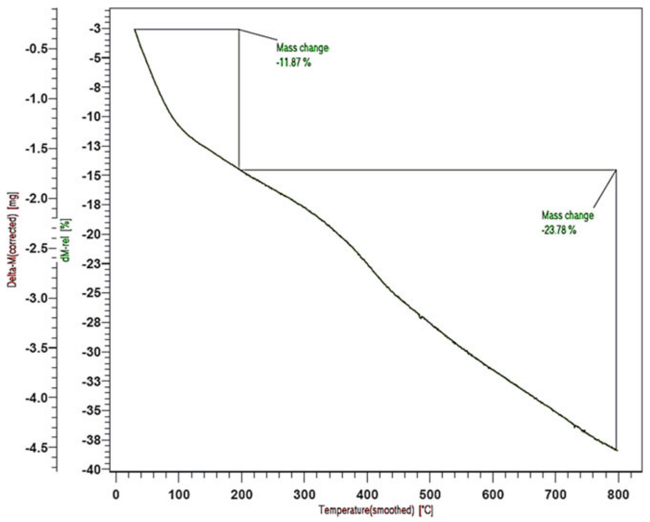

**FIGURE 6** TGA thermogram of MCM-41-Crown nanocomposite

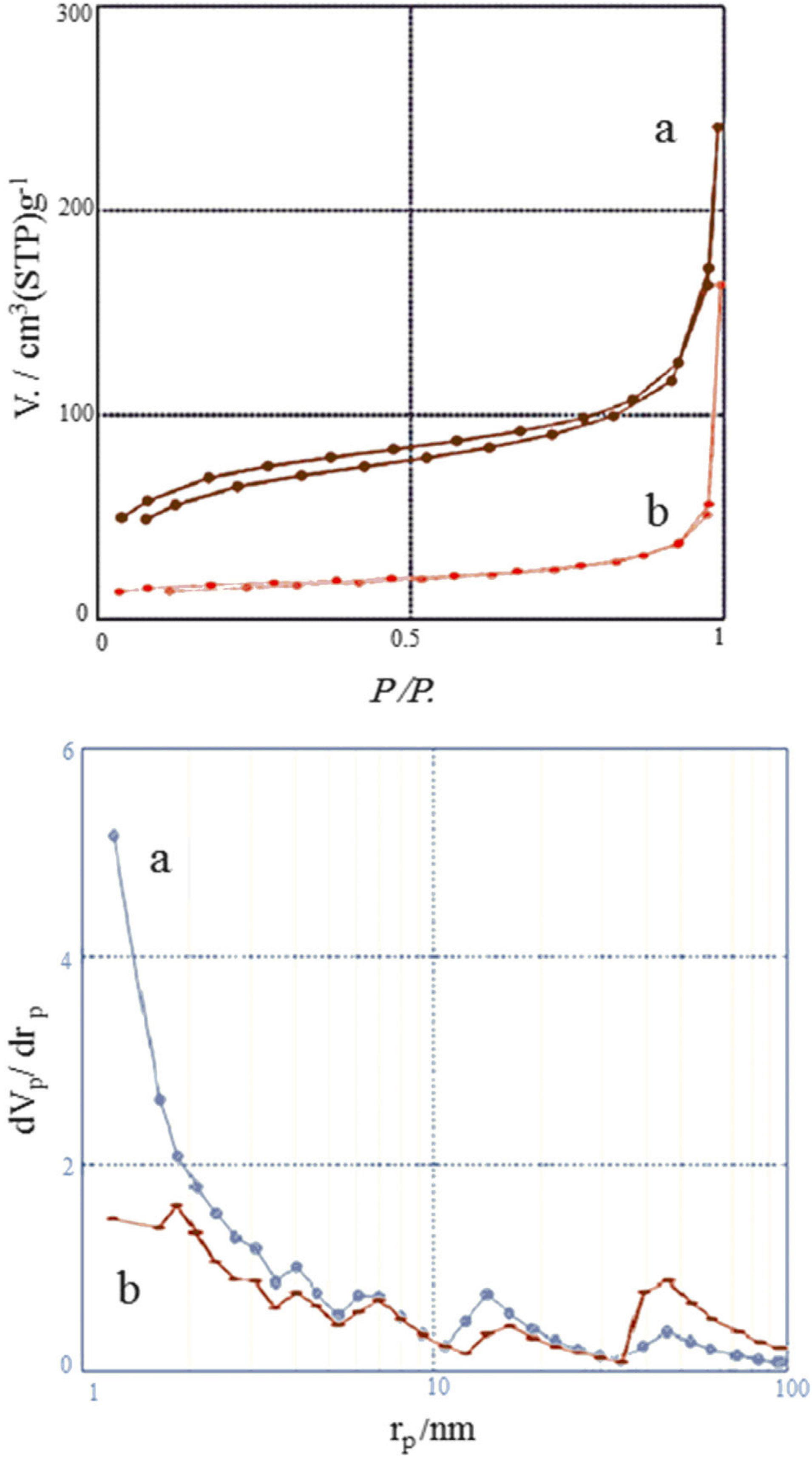

**FIGURE 7** Nitrogen adsorption–desorption isotherms (left) and pore size distributions (right) of (a) MCM-41-Crown and (b) MCM-41-Crown.Pd.

## 3 | RESULTS AND DISCUSSION

MCM-41-Crown.Pd was conveniently synthesized via the grafting of dibenzo-18-crown-6-ether moieties on the MCM-41 surface by surfactant-templated sol–gel methodology and post-modification process, followed by reaction of the resulting MCM-41-Crown with palladium acetate and then reduction in ethanol.[38,39] The systematic steps of MCM-41-Crown.Pd preparation are shown in Scheme 1.

To characterize the nanocomposite, and to confirm the immobilization of the active components on the pore surface of MCM-41, FT-IR spectroscopy was utilized (Figure 1). In all spectra, the typical Si—O—Si bands at around 1212, 1080, 795 and 462 cm$^{-1}$ associated with the formation of a condensed silica network are present, but a weak peak associated with Si—OH groups at 964 cm$^{-1}$ is also present, and peaks appearing at 2916 and 2851 cm$^{-1}$ are characteristic of C—H stretching vibrations. A broad band at 3100 to 3600 cm$^{-1}$ and a weak band at around 1520 cm$^{-1}$ observed in the spectrum of MCM-41-NH$_2$ are attributed to NH$_2$ stretching vibrations, indicating the presence of amino-functionalized groups in MCM-41-NH$_2$. In addition, the FT-IR spectrum of MCM-41-Crown exhibits a new peak at 1682 cm$^{-1}$ which is assigned imine band and confirms that DFBCE was covalently grafted onto the surface of MCM-41-NH$_2$.

SEM was used to determine the particle size and particle morphology. Figure 2 shows SEM images of MCM-41, MCM-41-Crown and MCM-41-Crown.Pd composite, indicating spherically shaped morphology without intergrowth aggregation and monodisperse and regular uniform nanoparticles. The particles exhibit a size distribution from 300 to 500 nm with an average size of around 350 nm.

TEM studies of the MCM-41-Crown and MCM-41-Crown.Pd organic–inorganic composites (Figure 3) revealed that the Pd nanoparticles had been incorporated successfully in the mesoporous organosilica. Some dark spots appearing on the surface of MCM-41-Crown.Pd can be attributed to the presence of Pd nanoparticles on the support matrix, shown with arrows in Figure 3. The nanocomposite morphology is close to spherical and the particle size of Pd(0) is around 11 nm which is near to the value calculated from XRD data.

The EDS analysis (Figure 4) of the nanocomposite shows the elements, including C, O, N and Si, that are present in the structure of the nanocomposite. In addition, the presence of palladium is indicated on MCM-41-Crown.Pd. The incorporation of Pd(0) in the nanocomposite was also confirmed and determined (2 wt%) using AAS.

The UV diffuse reflectance spectrum (S7, supporting information) showed complete conversion of Pd(II) to Pd(0) by the absence of a peak at 420 nm of the Pd(II) species.[40–42] To confirm the crystallinity of the Pd nanoparticles, the sample was characterized using XRD analysis (Figure 5a). The result reveals the presence of Pd nanoparticles on the silica surface with characteristic peaks at $2\theta$ of 40.0°, 46.9°, 67.9° and 80.1° corresponding to [111], [200], [220] and [311], respectively, and the strongest peak of the XRD pattern corresponding to the structure of silica phase. This observation confirms the presence of metallic Pd particles on the mesoporous MCM-41 surface.[15] The low-angle XRD pattern of the MCM-41-Crown.Pd nanocomposite (Figure 5b) shows one peak at $2\theta = 2.6°$, corresponding to the [100] plane, which is characteristic of a hexagonal pore system. The size of the Pd nanoparticles is estimated as 12 nm using the Scherrer equation.

TGA was used to determine the percentage of organic functional groups chemisorbed onto MCM-41. The TGA curve of MCM-41-Crown shows the mass loss of the organic materials as they decompose upon heating (Figure 6). According to this curve, there are two weight loss steps. The first weight loss is of 11.87% below 200 °C which might be due to the loss of physically adsorbed water as well as dehydration of the surface OH groups and organic solvents. The second weight loss step of about 23.78% in the range 200–800 °C is due to thermal decomposition of organic parts, and probably the condensation of the silanol groups of the silica shell. Thus, TGA also confirms the successful grafting of crown ether onto the surface of mesoporous MCM-41. The total weight loss over the full temperature range is estimated to be 35.65% due to the loss of the adsorbed water and organic units.

**TABLE 1** Comparison of textural parameters of MCM-Crown and MCM-41-Crown.Pd

| Sample | BET surface area (m$^2$ g$^{-1}$) | Pore volume (cm$^3$ g$^{-1}$) |
|---|---|---|
| MCM-Crown | 225 | 3.66 |
| MCM-41-Crown.Pd | 162 | 1.38 |

**TABLE 2** Optimization of MCM-41-Crown.Pd nanocomposite in proposed reaction

| Entry | Catalyst (mg) | Base (mmol) | Time (min) | Yield (%) |
|---|---|---|---|---|
| 1 | — | 2.5 | 360 | — |
| 2 | 40 | 2.5 | 45 | 70 |
| 3 | 50 | 2.5 | 25 | 80 |
| 4 | 70 | 2 | 30 | 80 |
| 5 | 70 | 2.5 | 25 | 98 |

Figure 7 shows the low-temperature nitrogen adsorption–desorption isotherms and pore size distributions of MCM-41-Crown and MCM-41-Crown.Pd nanocomposites. MCM-41-Crown (Figure 7a) exhibited a type-IV isotherm with sharp capillary condensation steps at relative pressure ($P/P_0$) range and an H1-type narrow hysteresis loop, which is typical of mesoporous solids. The hysteresis loops are very narrow, which clearly indicates the narrow channels of the MCM-41 mesoporous support.[43] But as shown in Figure 7(b), MCM-41-Crown.Pd exhibits a type-III isotherm. Regarding the synthetic strategy of nanocomposite synthesis, in the aminopropyl grafting step, pores of MCM-41 were occupied by the surfactant. Because of this, a large amount

**TABLE 3** Heck cross-coupling reactions catalysed by MCM-41-Crown.Pd nanocomposite

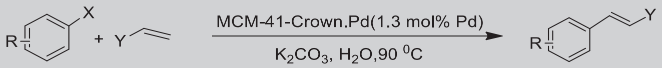

| Entry | R | X | Y | Time (min) | Yield (%)[a] |
|---|---|---|---|---|---|
| 1 | H | I | Ph | 25 | 92 |
| 2 | H | I | $CO_2H$ | 30 | 90 |
| 3 | 4-$NO_2$ | I | Ph | 16 | 94 |
| 4 | 4-$NO_2$ | I | $CO_2H$ | 27 | 92 |
| 5 | H | Br | Ph | 60 | 85 |
| 6 | H | Br | $CO_2H$ | 90 | 89 |
| 7 | 4-OMe | Br | Ph | 40 | 75 |
| 8 | 4-OMe | Br | $CO_2H$ | 50 | 75 |
| 9 | 4-Me | Br | Ph | 53 | 87 |
| 10 | 4-Me | Br | $CO_2H$ | 70 | 85 |

[a] Reaction conditions: 1 mmol of aryl halide, 1 mmol of terminal alkene, 5 ml of $H_2O$, 0.07 g of MCM-41-Crown.Pd and 2.5 mmol of $K_2CO_3$.

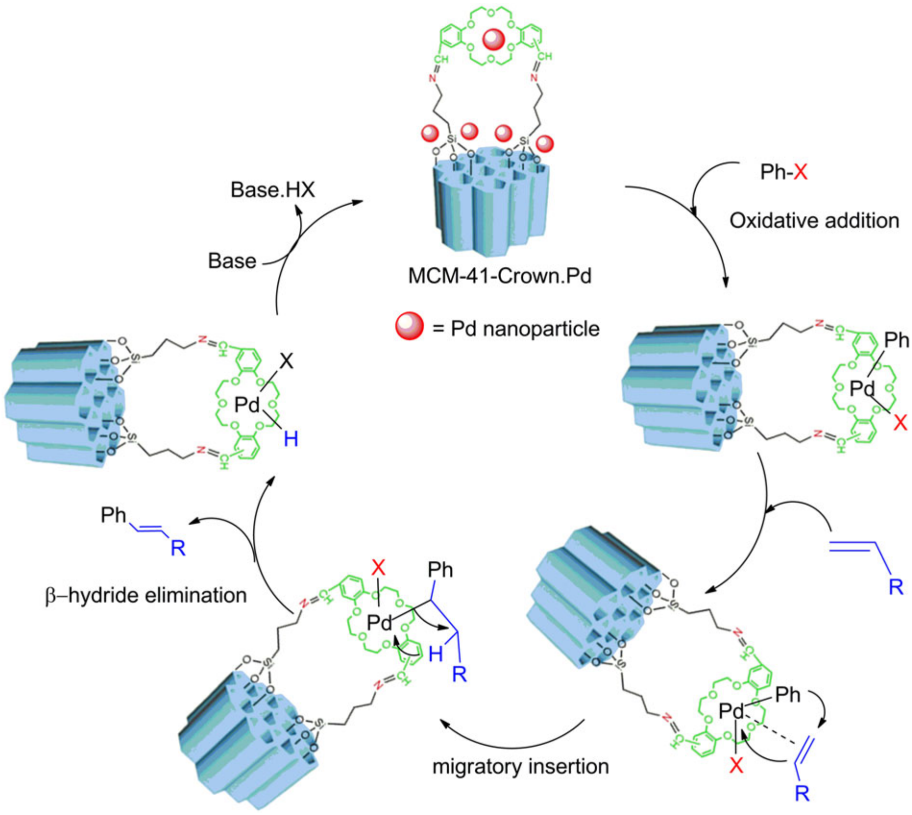

**SCHEME 2** Plausible reaction mechanism for Heck reaction catalysed by MCM-41-Crown.Pd.

of grafting units were dispersed onto the MCM-41 surface and some of them were trapped in the interior of MCM-41, and so consequently surface area and pore volume of MCM-41-Crown were reduced.

Some important data of Brunauer–Emmett–Teller (BET) surface area and pore volume of MCM-41-Crown and MCM-41-Crown.Pd are presented in Table 1. As a result of the Pd nanoparticles depositing inside the cavities of the crown ether and onto the surface of MCM-41, there is a decrease in surface area and pore volume.[44,45]

To evaluate the catalytic activity of MCM-41-Crown. Pd as a reusable and heterogeneous porous inorganic–organic hybrid nanocatalyst and with an aim of developing a simple practical method for carbon–carbon bond formation through Heck coupling reactions, initially the reaction of iodobenzene (1 mmol) and styrene (1 mmol) in the presence of $K_2CO_3$ and the nanocomposite was selected as a model system in aqueous medium under thermal conditions (90 °C). According to TLC, only one spot of alkene product was produced after 25 min. Optimization of a number of reactants and the catalyst showed that 2.5 mmol of $K_2CO_3$ and 0.07 g of the catalyst completed the reaction in the minimum time (Table 2). It is worth mentioning that the reaction in the absence of nanocomposite after prolonged reaction time did not afford any product.

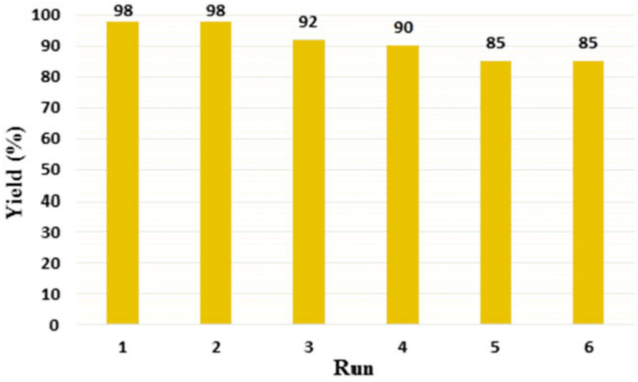

**FIGURE 8** Recyclability of nanocatalyst

The generality and synthetic scope of this coupling protocol were demonstrated by synthesizing a series of stilbenes in 25–90 min and in yields of 75–94%. As clearly evident from Table 3, the MCM-41-Crown.Pd nanocomposite can catalyse the Heck cross-coupling reactions of various aryl halides containing electron-withdrawing and electron-donating groups with styrene and acrylic acid.

The cavity size of the crown ether is 2.6–3.2 Å in diameter. Hydrophilic Pd(0) atoms have a radius of 1.37 Å, which makes them suitable for enclosure in the crown cavity. Further, the crown has an open structure, and thus can allow Pd(0) orbitals to engage in the Heck coupling reaction. A plausible reaction mechanism for the Heck coupling reaction is shown in Scheme 2, giving us a general picture of the steps needed for catalytic olefination. The first step is oxidation addition of Pd(0) catalyst to afford σ-arylpalladium(II) complexes. Coordination of the terminal alkene and subsequent C—C bond formation by syn addition provide σ-alkylpalladium(II) intermediates which readily undergo β-hydride elimination to release the alkene Heck product. For the continuance of the cycle, a base ($K_2CO_3$) is needed for the conversion of

**TABLE 4** Comparison of results of present system with those of some recently reported procedures

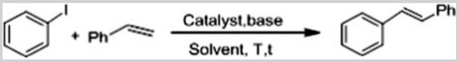

| Entry | Catalyst and conditions | Yield | Ref. |
|---|---|---|---|
| 1 | MCM-41-Pd, $Bu_3N$, NMP, 100 °C, 72 h | 95 | [49] |
| 2 | MCM-41-S-Pd(0), $Bu_3N$, NMP, 100 °C, 6 h | 98 | [50] |
| 3 | NHC-Pd/MCM-41[a], DMA/$H_2O$, 130 °C, 2 h | 96 | [18] |
| 4 | MCM–$NH_2$·Pd(0), $Et_3N$, DMF, 70 °C, 2 h | 95 | [19] |
| 5 | Pd(0)-MCM-41, DMF, NaOAC, 100 °C, 24 h | 90 | [20] |
| 6 | Pd-MCM-41, NMP, $Na_2CO_3$, 150 °C, 1 h | 84 | [21] |
| 7 | MCM-41-2P-Pd(0)[b], $Bu_3N$, NMP, 100 °C, 5 h | 94 | [39] |
| 8 | MCM-41-SH-Pd(0), $Bu_3N$, NMP, 100 °C, 6 h | 92 | [22] |
| 9 | PdNP-SβCD[c], $K_2CO_3$, $H_2O$, 90 °C, 2 h | 98 | [38] |
| 10 | MCM-41-Crown.Pd, $K_2CO_3$, $H_2O$, 90 °C, 0.4 h | 98 | This work |

[a] MCM-41-supported N-heterocyclic carbene–Pd complex.

[b] Diphosphino-functionalized MCM-41-anchored palladium (0) complex.

[c] Pd nanoparticles on silica β-CD substrate.

hydridopalladium(II) complex [HPdXL] to the active Pd(0) catalyst. This mechanism is proposed based on reported literature.[46–48]

Reusability is one of the most important benefits of heterogeneous catalytic systems from economic and environmental points of view. The recyclability of the nanocomposite was investigated for the reaction between iodobenzene and styrene by carrying out seven consecutive cycles using the same reaction conditions. After each run, the catalyst was easily recovered by vacuum filtration using Whatman filter paper, then washed with $Et_2O$ (5 ml) and *n*-hexane (5 ml). The solid catalyst was dried under vacuum after each cycle and then reused for the next reaction (Figure 8).

In view of the leaching problems observed with palladium supported on MCM-41-Crown, quantitative analysis using AAS was employed to determine the amount of metal in the reaction. The heterogeneity of the MCM-41-Crown.Pd catalyst was examined by carrying out a hot filtration test using styrene and iodobenzene as model substrates. No palladium could be detected in the liquid phase using AAS and, more significantly, after hot filtration, the reaction of the residual mixture was completely stopped.

To demonstrate the superiority of MCM-41-Crown.Pd over previously reported catalysts, the reaction of iodobenzene and styrene was considered as a representative example (Table 4). In all of these cases, comparative yields of the desired product were obtained following the MCM-41-Crown.Pd-catalysed procedure. These results clearly show that the nanocomposite is an equally or more efficient catalyst for this reaction.

## 4 | CONCLUSIONS

In this study, we fabricated a novel nanocatalyst architecture of Pd nanoparticles (1.3 mol% Pd) loaded into mesoporous organosilica (MCM-41-Crown) via surfactant-templated sol–gel methodology and then post-modification process. The Pd nanoparticles were synthesized from the ambient temperature reduction of $Pd(OAc)_2$ in ethanol under anhydrous conditions. It was found that the novel heterogeneous nanocatalyst is a highly efficient, stable and recyclable catalyst for the Heck cross-coupling reaction in water at 90 °C using $K_2CO_3$. The experimental results showed that the MCM-41 surface modified by dibenzo-18-crown-6-ether can improve the catalytic performance of the Pd nanoparticles. Furthermore, the catalyst can be recovered by simple filtration from a reaction mixture and reused for seven consecutive runs with a moderate decrease in product yield, and promises economic as well as environmental benefits.

## ACKNOWLEDGEMENT

This work was supported by the Research Council at the Shahid Chamran University of Ahvaz.

## ORCID

*Maedeh Azaroon* http://orcid.org/0000-0002-6867-3418

## REFERENCES

[1] H. Hattori, K. Otsuka, *Science and Technology in Catalysis*, Elsevier Science **1999**.

[2] K. Moller, B. Thomas, *Chem. Mater.* **1998**, *10*, 2950.

[3] M. D. Alba, L. Zhaohua, J. Klinowski, *J. Phys. Chem. A* **1996**, *100*, 2178.

[4] R. Nejat, M. Chamack, A. Mahjoub, *Appl. Organometal. Chem.* **2017**, *31*, 3745.

[5] W. Hao, G. Ding, M. Cai, *Catal. Commun.* **2014**, *51*, 53.

[6] E. Vasile, F. Dumitru, A. Razvan, O. Oprea, C. Andronescu, *Dig. J. Nanomater. Biostruct.* **2013**, *8*, 433.

[7] C. J. Pedersen, *J. Am. Chem. Soc.* **1967**, *89*, 7017.

[8] S. Yousefi, A. R. Kiasat, *RSC Adv.* **2015**, *5*, 92387.

[9] M. Ouchi, Y. Inoue, Y. Liu, *Bull. Chem. Soc. Jpn.* **1990**, *63*, 1260.

[10] F. Hoffmann, M. Cornelius, J. Morell, M. Fröba, *Angew. Chem.* **2006**, *45*, 3216.

[11] H. Keypour, S. G. Saremi, M. Noroozi, H. Veisi, *Appl. Organometal. Chem.* **2017**, *31*, 3558.

[12] M. Yoosefian, Z. Ansarinik, N. Etminan, *J. Mol. Liq.* **2016**, *213*, 115.

[13] M. Yoosefian, N. Etminan, *RSC Adv.* **2016**, *6*, 64818.

[14] A. Khalafi-Nezhad, F. Panahi, *Green Chem.* **2011**, *13*, 2408.

[15] G. Z. Fan, S. Q. Cheng, M. F. Zhu, X. L. Gao, *Appl. Organometal. Chem.* **2007**, *21*, 670.

[16] S. Rahmati, A. Arabi, A. Khazaei, M. Khazaei, *Appl. Organometal. Chem.* **2016**, *31*, 1.

[17] X. Fei, W. Kong, X. Chen, X. Jiang, Z. Shao, J. Y. Lee, *ACS Catal.* **2017**, *7*, 2412.

[18] S. M. Sarkar, M. M. Yusoff, M. L. Rahman, *J. Chin. Inst. Chem.* **2015**, *62*, 33.

[19] J. Zhou, R. Zhou, L. Mo, S. Zhao, X. Zheng, *J. Mol. Catal. A* **2002**, *178*, 289.

[20] S. Jana, B. Dutta, R. Bera, S. Koner, *ACS Appl. Mater. Interfaces* **2008**, *47*, 5512.

[21] A. Papp, G. Galbács, Á. Molnár, *Tetrahedron Lett.* **2005**, *46*, 7725.

[22] Q. Xu, M. Cai, *Catal. Commun.* **2007**, *67*, 515.

[23] A. Balanta, C. Godard, C. Claver, *Chem. Soc. Rev.* **2011**, *40*, 4973.

[24] M. Yoosefian, N. Etminan, *RSC Adv.* **2015**, *5*, 31172.

[25] M. Yoosefian, H. Raissi, A. Mola, *Sens. Actuators B* **2015**, *212*, 55.

[26] N. Etminan, M. Yoosefian, H. Raissi, M. Hakimi, *J. Mol. Liq.* **2016**, *214*, 313.

[27] M. Yoosefian, N. Etminan, *Phys. E* **2016**, *81*, 116.

[28] M. Yoosefian, *Appl. Surf. Sci.* **2017**, *392*, 225.

[29] M. Yoosefian, A. Mola, E. Fooladi, S. Ahmadzadeh, *J. Mol. Liq.* **2017**, *225*, 34.

[30] H. M. Hassan, E. M. Saad, M. S. Soltan, M. A. Betiha, I. S. Butler, S. I. Mostafa, *Appl. Catal. A* **2014**, *488*, 148.

[31] M. Nikoorazm, F. Ghorbani, A. Ghorbani-Choghamarani, Z. Erfani, *Chin. J. Catal.* **2017**, *38*, 1413.

[32] C. Xu, Y. Lin, B. Huang, H. Liu, M. Cai, *Tetrahedron* **2016**, *72*, 2065.

[33] W. Hao, D. Guodong, C. Mingzhong, *Catal. Commun.* **2014**, *51*, 53.

[34] B. W. Glasspoole, D. W. Jonathan, M. C. Cathleen, *J. Catal.* **2009**, *265*, 148.

[35] M. Cai, J. Sha, *Catal. Commun.* **2007**, *11*, 1691.

[36] T. L. Yost, B. C. Fagan, L. R. Allain, C. E. Barnes, S. Dai, M. J. Sepaniak, Z. Xue, *Anal. Chem.* **2000**, *72*, 5516.

[37] A. Khazaei, M. K. Borazjani, K. M. Moradian, *J. Chem. Sci.* **2014**, *124*, 1127.

[38] A. Khalafi-Nezhad, F. Panahi, *ACS Sustain. Chem. Eng.* **2014**, *2*, 1177.

[39] P. D. Burton, T. J. Boyle, A. K. Datye, *J. Catal.* **2011**, *280*, 145.

[40] M. Gholinejad, F. Hamed, P. Biji, *Dalton Trans.* **2015**, *44*, 14293.

[41] H. Firouzabadi, N. Iranpoor, M. Gholinejad, S. Akbari, N. Jeddi, *RSC Adv.* **2014**, *4*, 17060.

[42] M. Khan, G. H. Albalawi, M. R. Shaik, M. Khan, S. F. Adil, M. Kuniyil, H. Z. Alkhathlan, A. Al-Warthan, M. R. H. Siddiqui, J. Saudi, *Chem. Soc.* **2017**, *21*, 450.

[43] C. M. Lin, T. L. Hung, Y. H. Huang, K. T. Wu, M. T. Tang, C. H. Lee, C. Chen, Y. Chen, *Phys. Rev. B* **2007**, *75*, 125426.

[44] H. Yoshitake, T. Yokoi, T. Tatsumi, *Chem. Mater.* **2002**, *14*, 4603.

[45] H. Yang, G. Zhang, X. Hong, Y. Zhu, *J. Mol. Catal. A* **2004**, *210*, 143.

[46] N. Noori, M. Nikoorazm, A. Ghorbani-Choghamarani, *J. Porous Mater.* **2016**, *23*, 1467.

[47] I. Bucsi, Á. Mastalir, Á. Molnár, K. L. Juhász, A. Kunfi, *J. Struct. Chem.* **2017**, *28*, 501.

[48] A. Kumbhar, *Top. Curr. Chem.* **2017**, *2*, 375.

[49] F. Y. Tsai, C. L. Wu, C. Y. Mou, M. C. Chao, H. P. Lin, S. T. Liu, *Tetrahedron Lett.* **2004**, *45*, 7503.

[50] M. Cai, Q. Xu, J. Jiang, *J. Mol. Catal. A* **2006**, *260*, 190.

## SUPPORTING INFORMATION

Additional Supporting Information may be found online in the supporting information tab for this article.

**How to cite this article:** Azaroon M, Kiasat AR. An efficient and new protocol for the Heck reaction using palladium nanoparticle-engineered dibenzo-18-crown-6-ether/MCM-41 nanocomposite in water. *Appl Organometal Chem*. 2018;e4271. https://doi.org/10.1002/aoc.4271